

Manuscript published in Journal of Archaeological Science 2017, 81, 1-12.

Iridium to provenance ancient silver

Jonathan R. Wood, Michael F. Charlton, Mercedes Murillo-Barroso, Marcos Martín-Torres

Institute of Archaeology UCL, 31-34 Gordon Square, London WC1H 0PY, UK.

ABSTRACT

Trace levels of iridium in ancient silver artefacts can provide information on the sources of silver-bearing ores as well as the technologies used to extract silver. A geographically and chronologically disparate legacy dataset, comprised of Near Eastern objects from the Sasanian and Byzantine Empires (1st Millennium AD) and coins circulating around the Mediterranean in the mid-1st Millennium BC, shows that Ag-Au-Ir log-ratio plots can help identify silver derived from the same mining areas, as well as broadly differentiating between the ore types exploited. Combining trace element and lead isotope analyses through the Pb crustal age of the ore, further delimits interpretations on the compositions and locations of silver ore sources. Furthermore, it is shown that silver artefacts of Near Eastern origin have exceptionally high iridium levels, suggesting a unique silver-bearing ore source, potentially in the Taurus mountain range of southern Anatolia. The wide range of crustal ages identified for ancient Greek coins and Near Eastern objects suggest that the addition of exogenous lead as a silver collector during smelting was common practice in the Near East as early as 475BCE. The practice of mixing silver from different sources has also been identified by triangulating the log-ratio subcomposition plots, Pb crustal ages of the ore from which the silver derived and absolute values of trace levels of gold and iridium in silver artefacts.

Keywords

Ancient silver; Provenance; Legacy data; Iridium; Lead isotope analysis; Trace elements; Mixing silver

1. INTRODUCTION

Metal ores are unevenly distributed over large areas, which suggests some kind of long-distance transport is required to explain the geographical distribution of artefacts in the archaeological record (Pernicka, 2014). Tracing the ore source of ancient metal artefacts can complement any investigations based on style and iconography, thereby providing information on the movement of the materials that culminated in final deposition of the object.

Provenancing silver objects has been attempted since the 19th century using elemental analyses and more recently using lead isotope ratios (for a review, see Pernicka, 2014). In order to determine the trajectory of a silver object from its ore source, a metallurgical signature needs to be identified and measured (Randle et al., 1973 ; Meyers et al., 1975). Establishing a relation between chemical analyses on ancient silver objects and mineralogical sources of silver requires not only knowledge of the composition of the ores, but also of how the composition changes during smelting and cupellation (a selective oxidation process where silver is separated from its less-inert lead host) (Pernicka et al., 1998). For example, a silver-bearing ore, such as galena (PbS) or cerussite (PbCO₃), contains, in addition to lead, a small amount of silver but a large number of impurities. Some of these elements are retained in the silver, while others are partially or completely removed into slag or fumes during the smelting and refining processes (McKerrel and Stevenson, 1972; Pernicka and Bachmann, 1983 ; L'Heritier et al., 2015). Furthermore, contamination can occur from materials used in furnaces, fuel and fluxes. Deliberate additions to the system, such as alloying elements or recycled silver from other sources, contain their own associated impurities which can also contribute to the final composition of the silver object, thus potentially blurring further the provenance signature. Exogenous lead, added as a silver collector during extraction from lead-poor silver-bearing ores, affects the lead isotope signature derived from the silver and may render the provenancing of archaeological silver even more challenging than for other materials (Murillo-Barroso et al., 2016).

The complexity of the processes involved in the production and alloying of silver makes determining a parent-ore indicator extremely challenging, especially when it is considered that any indicator needs to have significant variability between ore sources. In other words, not only does an indicator need to survive the smelting, cupellation and alloying operations, but also the variability within a single ore source must be small compared to variations in geographically separated ore sources (Pollard and Bray, 2015).

Trace levels of gold in silver have been considered associated solely with silver sources, as they tend to be virtually absent in any other material in the system and they are not significantly altered by the smelting and cupellation processes (Gitler et al., 2009). Variability in gold concentrations between silver artefacts has been applied successfully to differentiate between lead ore types (the main source of ancient silver), with an empirical value of 0.1 wt% Au in silver objects being the upper limit for galena ore sources (Pernicka, 1981). Iridium (Ir), like gold, is an inert siderophile element (Alard et al., 2000). Traces of iridium have been found in ancient silver artefacts, suggesting that this metal with its high melting point (2447 °C) and similar atomic size to silver survives the smelting and cupellation process (Ogden, 1977). Furthermore, gold and iridium are unlikely to enter the system in any significant amount due to alloying (i.e. copper, the main alloying metal is poor in these elements and rarely exceeds more than 5 wt% of the silver alloy) or to be associated with any non-argentiferous lead (a chalcophile) added as a exogenous silver collector in the smelting of lead-poor silver-bearing ores. Hence gold and iridium are potential proxies to provenance silver from ore to object.

This paper aims to further this hypothesis through the re-analysis of a legacy dataset of 283 analyses on silver objects together with published data on ores. We propose that Ag-Au-Ir log-ratio plots are useful to discriminate silver deriving from different ore types, hence contributing to provenance studies, and that sometimes iridium levels alone can be very diagnostic of individual sources. In addition, we explore new ways of combining this information with lead isotopic data, leading to more robust approaches to the identification of exogenous lead additions for silver extraction, silver mixing through recycling, and metal fingerprinting generally.

2. LEGACY DATA AND RE-ANALYSIS

Although iridium is not measured routinely in archaeometallurgy, some studies have measured iridium without using it explicitly as a discriminator (Gale et al., 1980). Other investigations, especially those associated with Pieter Meyers, were quite successful at grouping silver artefacts using iridium, often with an aim of assessing the authenticity of silver objects in museum collections (Harper and Meyers, 1981 ; Meyers, 1992). Meyers' experimental analysis on Sasanian silver (Harper and Meyers, 1981) measured major, minor and some trace elements (including iridium) in 38 objects from several museums around the world. Although un-provenanced, these objects are made of silver from potentially a single ore source (see Section 2.2). Similarly, a study on ecclesiastical Byzantine silver provides compositional data from 69 objects dated between the 4th and 7th centuries AD (Meyers, 1992). Several of these objects were later analysed for lead isotopes (LIA) in a study with two other artefacts in order to investigate their authenticity as ancient objects (Scott, 1990). A numismatic study on the Asyut hoard (pre-475BCE) measured iridium concentrations in 283 coins, 102 of which have associated LIA data (Gale et al., 1980 ; Stos-Gale and Gale, 2009). The mints of some of these coins have been suggested, which provide a potential indication of the ore source of silver, since silver from the Athenian mint is generally accepted to have come from the mines at Laurion on the Attic peninsula.

The following re-analysis has simply pooled this data with no particular archaeological question: our hypothesis is largely methodological, even if our results may be useful for later archaeological discussion (which is not attempted here). We believe this data set includes the majority of analyses in which iridium was measured for archaeological silver, some of which have associated LIA measurements. The focus is on the ore sources which, in some cases, may have been the same, irrespective of the period. Hence, we believe that the use of an archaeologically disparate dataset is justified. All compositional legacy data presented in the current study were measured using neutron activation analysis (NAA) or inductively coupled plasma mass spectrometry (ICP-MS). All compositional and LIA data used can be found in Supplementary Table 1.

Fig. 1 presents histograms of Au and Ir concentrations for this chronologically and geographically disparate dataset. The gold distribution appears to be bi-modal. The gold concentration in silver is often used to differentiate silver which originated from non-galena (>0.1 wt% Au) and galena ore (<0.1 wt% Au) sources (Pernicka, 1981). Iridium has a skewed distribution with a median value of 44 ppb.

A re-analysis of this legacy data has been conducted treating the system as a series of sub-compositional components, by transforming the data to a log-ratio scale (Aitchison, 1986 ; Aitchison, 2005). This approach removes the effects of the constant sum constraint (which compels the data to lay between 0 and 100%) in order to eliminate any 'spurious correlations' (Chayes, 1949). In essence, it considers from the outset that the interest lies in the relative magnitudes and

variations of components, instead of in their absolute values. A multivariate analysis was performed of the full chemical data set using the Compositions package in R created by van den Boogaart (2013), applying Aitchison's geometry (i.e. the centred log-ratio transformation) to the raw compositional data. After using the variation matrix to measure the spread in the compositional data, the subcomposition Ag-Au-Ir was identified as providing the ratios which best represented the full composition. Log-ratio plots (e.g. Fig. 2) were constructed using the raw data of each component in the subcomposition, i.e. $\log(\text{Ag/Ir})$ and $\log(\text{Au/Ir})$.

2.1 SASANIAN SILVER

In the original study (Harper and Meyers, 1981), Sasanian compositional data was split into specific groups delineated by style, shape and iconography. Four vessel groups were identified: 1) early Sasanian bowls or plates, 2) central Sasanian hunting plates, 3) provincial hunting plates, 4) provincial bowls or plates with enthronement scenes. The central Sasanian hunting plates were produced in the paired-line drapery style, with kings wearing correctly rendered Sasanian crowns, indicating that they were made onward from the time of Shapur II (309-379AD) up until the 6th or 7th century AD. The authors concluded that there existed both a central Sasanian, royal production, subject to state controls, and several independent, provincial industries that were the source of a related class of vessels. Since it is not the intention of the current re-analysis to investigate phases of Sasanian iconography, but to identify the utility of a method on a dataset from a well-defined region (as well as to avoid any circular arguments regarding artefacts where both style and composition appear to have contributed to their grouping), the central Sasanian hunting plates were placed in one group (referred to here as Sasanian-Royal - red points), while all others were placed in another (Sasanian - blue points). One analysis from the central Sasanian hunting plates, focussing on an ancient repair (with silver), was coded separately (Sasanian-Royal-Repair - purple point).

Fig. 2a shows a centred ternary diagram for the Ag-Au-Ir subcomposition on a dimensionless scale. The data appear to show a one dimensional pattern suggesting that the ratio involving Au and Ag has an almost constant value, and that most compositional variance is due to variability of Ag/Ir and Au/Ir, i.e. $(\text{Au/Ir}) = k (\text{Ag/Ir})$, or $\log (\text{Au/Ir}) = \log k + \log (\text{Ag/Ir})$. Furthermore, the central Sasanian hunting plates appear to cluster together.

This association becomes more evident when the data is plotted in terms of Ag-Au-Ir log-ratios (Fig. 2b). As Sasanian silver potentially derives from one mining area (see Section 2.2), it is proposed that the linearity of the plot reflects the variability of the subcomposition within the geological deposit from where the silver was extracted. It should be pointed out that this linearity is not a statistical artefact. In other words, the ratio of Au/Ir and Ag/Ir does not have to be constant unless there is some underlying association between the components. This claim is based on the similar premise used to interpret compositions of limestone deposits, where log-ratios of a subcomposition have demonstrated successfully that geochemically similar limestones across widely different regions have lithostratigraphic equivalence, irrespective of the geographical separation (Thomas and Aitchison, 2006), i.e. the subcomposition was shown to discriminate as effectively as the full composition (which often has 'noisy' components that ultimately contribute little information to the problem at hand). As such, it is suggested that the interaction in Fig. 2 identifies variability in dilution of chemically distinctive parts of the ore body, which results in systematic patterns of variability of a subcomposition retained through the processing operations from ore to object. In other words, the variability in the Au-Ag-Ir sub-composition of objects potentially discriminates between mining areas within an ore body.

Fig. 2b highlights that:

- Sasanian silver data is spread out, covering about six orders of magnitude on both axes on the log-ratio plot, mainly due to differences in the iridium concentrations.
- Data from the central Sasanian hunting plates (Sasanian-Royal) cover a much narrower range - about one order of magnitude.

The narrow range of the 'royal' Sasanian silver with respect to the other Sasanian silver objects, suggests they were made of silver from a specific mining area within a broader geological deposit, possibly a 'royal' mine. Furthermore, the composition of the ancient repair of a horse leg from a central Sasanian hunting plate (highlighted) suggests that not only was it made from silver that was extracted from a different mining area, but also from a different geological deposit, i.e. it is not only shifted with respect to the central Sasanian hunting plates, but it also appears to lie above the other data. Similarly, two points which lie below the other data (highlighted) are possibly from another geological deposit or a mixture of Sasanian silver with silver from another source.

2.2 BYZANTINE SILVER AND OBJECTS FROM GALENA ORE SOURCES

Fig. 3 shows that most Byzantine ecclesiastical artefacts appear to overlay the Sasanian data (now in grey).

This suggests that Byzantine silver derived from melting down Sasanian silver objects and/or Sasanian and Byzantine silver was mined from the same geological deposit, and in some instances, the same mining area. Meyers (1992) proposes an Anatolian source for the Byzantine silver. Mining at the Taurus mountain range of Southern Anatolia, although archaeologically unattested for this period, is a possible source of silver for both Byzantine and Sasanian silver, since both Empires had control over this region (Daryaee, 2009 ; Oates and Oates, 1959).

The highland regions of Anatolia are considered as one of the earliest environments in which metallurgy developed (Craddock, 1985 ; Tylecote, 1987) and are often cited as a likely source of raw materials such as metal, minerals and wood, critical to the populations in the resource-poorer environments of the Levant, Iraq and other areas of Anatolia (Muhly, 1973; Muhly, 1976; Charles, 1985 ; Moorey, 1985). For example, the Bolkardag valley of mines is 15 km long with numerous porphyritic dikes, due to natural processes and mining activities, irregular caves, cavities and tunnels. Massive secondary and detrital deposits of oxidised ores are found in these caves and cavities as well as abundant outcroppings (Yener et al., 1991), many showing signs of having been worked in antiquity (Yener and Özbal, 1986 ; Yener and Özbal, 1987). Some layered deposits have 100–1000 ppm of silver (and sometimes higher than 6000 ppm) as well as gold levels ranging between 1 and 100 ppm. The area has been described as polymetallic (Ayhan, 1984), mineralogically diverse (Yener et al., 1991) and as a highly complex geological zone (Sayre et al., 1992). Some areas of the Taurus mountains (e.g. Taurus 1A) have polymetallic ores rich in lead (10–30%), while others (e.g. Esendemirtepe) contain only modest amounts (1.2%) or very low lead concentrations (Yener et al., 1991). It has been proposed that mining in this region probably targeted argentiferous cerussite (PbCO₃) from the Bronze Age (Yener et al., 1991 ; Meyers, 1992) rather than the more demanding exploitation of galena, which tends to lie in deposits below the water table, and is consistently accompanied with the problematic sphalerite (ZnS) ores (Yener et al., 1991). The latter reduces the silver yield in addition to producing noxious fumes (SO₂) when smelted (Wertime, 1968 ; Wertime, 1973).

There is also evidence of silver extraction and cupellation in Iran during the Sasanian period (Meyers, 2003). However, the LIA signature (Nazafati and Pernicka, 2012) is different to that of the Byzantine

objects discussed here (suggesting that these Byzantine objects were not recycled from Sasanian objects derived from these ores). Furthermore, although LIA analyses have been conducted on Sasanian silver - unpublished data from Meyers (Stos-Gale, 2001) - which appear consistent with some Iranian deposits (e.g. Nakhlak), the limited number of LIA available makes it difficult to determine whether the majority of this silver is commensurate with Iranian ores. Moreover, some of this silver also falls within the LIA ore fields of the Taurus mountains. Thus, exploitation of silver deposits by the Sasanians in both Anatolia and Iran is highly probable, which further highlights the need for an approach which can help differentiate silver with similar LIA signatures.

Fig. 3 also plots the subcomposition of artefacts thought to be derived from galena ore sources, i.e. a group of Thraco-Macedonian coins from Orrescii (ca. 5th Century BC) minted in the vicinity of the galena ores of Mt Pangaeum (Gale et al., 1980) and silver from two Islamic silver plates for which a galena ore source has been suggested (Meyers, 2003). These data points clearly plot on a similarly sloped function, suggesting that the Ag-Au-Ir subcomposition has a similar variability within the silver of these lead ores, but with a lower y-offset than the Sasanian and Byzantine data. This is predominantly a consequence of the gold concentration, which is typically two orders of magnitude lower than found in silver derived from cerussite (see Fig. 1). This may relate to differences in the lithostratigraphic levels of the ore types, i.e. cerussite is often found close to the surface as a result of oxidation of the underlying galena and is therefore enriched in noble metals.

The plot in Fig. 3 also supports that 7thC AD Byzantine silver was potentially mined in a different area (although within the same geological deposit, hence the same alignment but slight separation) than 6thC AD Byzantine silver, that the contested Fisherman's (2-4thC AD?) and Philosopher's plate (4-6thC AD?) are consistent with the bulk of the dataset and hence likely Byzantine rather than from the Renaissance period (Scott, 1990), and that the Antioch Cross was probably made from silver from a completely different geological deposit (Meyers, 1992).

The log-ratio graph therefore has two main advantages over investigating the raw data alone: the clustering of data along discrete 'lines' suggests objects are from the same mining area (predominantly due to variations in the iridium concentrations); the intercept of the 'lines' reflect the type of ore, i.e. galena, cerussite etc. (predominantly as a consequence of the gold concentration in the silver). This suggests silver from ore types that are neither cerussite nor galena (or perhaps ores of various purities) would lay on different lines (as suggested by the ancient repair and the Antioch Cross).

2.3 ASYUT HOARD

Another set of data including trace elements comes from the work of Gale et al. (1980), who measured the composition of a number of coins from the Asyut hoard (and one coin from the Wells hoard), deposited in Egypt in about 475BCE. This hoard contains about 900 coins (283 elemental analyses were conducted of which 102 also have LIA data) and appears to be fairly representative of coins circulating around the Mediterranean at that time. The coins mainly come from Athens and Aegina, together with coins from Orrescii (plotted in Fig. 3), Thasos, Acanthus, Corinth, Lesbos, Samos, Mallus or Caria (Anatolia), Salamis (Cyprus), Lycia (Anatolia), Zankle and Messana (Sicily), Cyrenaica (Libya) and Persian sigloi (Sardes). The authors claim that the silver is unlikely to have been from mixed sources because of the limited use of coinage at this time - although this has been disputed (Jessop-Price, 1980) - and conclude from LIA data that there were three sources of silver: Laurion, Siphnos and an unidentified source.

A large number of the Asyut coins lay between the Sasanian/Byzantine and galena data lines. Fig. 4 shows the Asyut coin data, with the Sasanian and Byzantine data differentiated by using the gold

concentration of the silver, i.e. below 0.1%wt Au is considered to be a galena source (red), while above 0.1 wt% Au is a non-galena source (blue). The red line is a linear fit through the Orrescii (galena) data. The blue line is a linear fit of all the Sasanian and Byzantine (cerussite) data from Fig. 3. The silver coins which have greater than 0.1 wt% Au are unlikely to be from a galena source and therefore must derive from either cerussite or another non-galena ore (such as the complex sulphosalt silver ores of Siphnos) or from mixed silver. The cluster between the two lines at approximately $\log(\text{Ag}/\text{Ir}) = 19$ and $\log(\text{Au}/\text{Ir}) = 11$ contains the majority of the Athenian coins.

3. Pb CRUSTAL AGE

Some of the legacy data has associated lead isotope analyses (LIA), allowing a preliminary attempt to relate LIA with the trace amounts of iridium in silver. This is explored here through the estimated crustal age of the ore, as it combines three lead isotopes into one parameter (207Pb, 206Pb and 204Pb). It is not considered as a replacement for traditional lead isotope plots (which may allow variability in specific ratios to identify differences between objects and ores) but as an alternative that allows presenting on one plot the variability within lead isotope measurements alongside trace element data. For the data presented here (e.g. the Taurus mountains in Fig. 7), the Pb crustal age seems to be able to resolve ore deposits as effectively as the conventional 208Pb/206Pb versus 207Pb/206Pb plots (see Fig. 1 in Sayre et al., 1992).

Crustal ages were calculated from lead isotope data using a two-stage evolution model with the common Pb isotope composition and the $^{238}\text{U}/^{204}\text{Pb}$ of the crust (Stacy and Kramers, 1975; Albarède and Juteau, 1984 ; Desaulty et al., 2011). The calculations were performed using the approach outlined by Desaulty et al. (2011) and by applying their parameters to determine the model age. Different parameters are used by different groups of researchers, and the same groups often update the parameters they use (e.g. Albarède et al., 2012). However, the aim here is not to calculate crustal ages per se but to define a value for both the ore source and the associated object - both should have the same lead isotope ratios and hence the same calculated crustal age, whether or not this corresponds with an accurate geological age. In essence, the calculations are used to define a numerical value for both ore and object that allows them be compared, a value which is generally related to the crustal age of the ore body. This can lead to some ages producing negative values (i.e. future ages). This could mean that these leads have had a more complicated history than from the predicted rate of addition of radiogenic lead in the source region, during which they acquired extra amounts of radiogenic lead. Alternatively, it could mean that the model or the parameters are not refined sufficiently to represent the full range of ages. Nevertheless, for the purposes of this paper, the parameters used to calculate crustal ages for both the ores and objects were the same.

Fig. 5 shows a frequency distribution histogram of the Pb crustal ages (Ma) for the artefact dataset with associated LIA values. The lower crustal ages are commensurate with Laurion ores (Fig. 8). Peaks around 30, 60 and 95Ma suggest other ores sources, but could also suggest mixtures of silver sources or exogenous lead, each with their own respective lead isotopic signatures.

The Orrescii coins and a few of the Byzantine objects plotted in Fig. 3 have associated LIA data. It was anticipated that ores from the same geological deposit would have similar crustal ages, as would be expected if ore genesis occurs at similar times. This was not found to be the case. Fig. 6 shows that the Orrescii coins have Pb crustal ages within about 2 million years (Ma) of each other, strongly supporting the assumption that they come from a single mining area within a deposit (probably a young deposit in geological terms, and therefore consistent with Laurion). On the other hand, the

Byzantine silver objects, despite showing a relatively linear interaction on the sub-compositional log-ratio plot, have a wide range of crustal ages (about 100Ma).

The differences in crustal ages in the Byzantine objects could possibly be explained by the exploitation of different ores: Fig. 7 shows the variation in calculated crustal ages of ores from several areas in the Taurus mountains (LIA data from Yener et al., 1991; Wagner et al., 1992 ; Hirao et al., 1995), and it is apparent that just two mining deposits (Taurus 1B and 2A) could account for all the variability in the Byzantine silver dataset. In other words, the difference between the Orrescii and Byzantine crustal age data could be explained by considering that the tribe of Thraco-Macedonians who minted the Orrescii coins were more likely to exploit one area, while the Byzantine Empire had the potential to exploit multiple deposits. At the same time, the proximity of some of these Byzantine data points to each other on the log-ratio plot might lead to the expectation that their crustal ages should also be similar (i.e. the same mining area should have the same crustal age). The observation that they do not suggests that one of the geological models is not appropriate: either the hypothesis that silver objects which group together on the log-ratio plot (Fig. 3; Fig. 5) are from the same mining area, or that the crustal age represents the deposit from which the silver was extracted. This is explored further in the discussion section.

Regarding the Asyut hoard, the histogram (Fig. 8) shows that the range of crustal ages for Laurion ores (from over 15 mining sites at Laurion) correspond well with the range of ages from the Athenian coins (LIA data from Stos-Gale et al., 1996 ; Chalkias et al., 1988). In terms of average crustal ages, the Athenian and Orrescii coins are similar. This implies that in order to differentiate between these two sources the sub-compositional log-ratio plot is required, which shows that the Orrescii data lie on a slope with a lower y-offset than the Laurion data (i.e. Fig. 4) potentially because the purity of galena is different at these two locations.

Pb crustal age (Ma) was plotted against $\log(\text{Au}/\text{Ir})$ and $\log(\text{Ag}/\text{Ir})$ on a kernel density plot for the Asyut coin data (Fig. 9), where the shading corresponds to the smallest region that contains the respective probability. Two regions of higher density can be observed on the Pb crustal age vs. $\log(\text{Au}/\text{Ir})$ plot. The lower region corresponds well with silver from Laurion. The higher crustal age zone is more diffuse and absent in the Pb crustal age vs. $\log(\text{Ag}/\text{Ir})$ plot, which suggests a greater spread of crustal ages. Consequently, several sources in the Aegean (and further afield) correspond to this range. This is one of the main issues with any inferences based on LIA data alone, i.e. LIA fields often overlap (as in Fig. 7). The spread also suggests that the majority of coins are not purely from two or three ore sources (Gale et al., 1980).

4. EXAMINING IRIDIUM LEVELS

So far we have focussed on the relative magnitudes and variations of our elements of interest as the most useful proxy to approach silver provenance. Here we turn briefly to the absolute iridium levels in the silver as an indicator that may also be useful in some cases.

Table 1 shows absolute amounts of iridium (ppb) against the Pb crustal age (Ma) for all the data ($n = 283$) and those with associated LIA ($n = 102$). The data has been separated into four groups based entirely on geographical considerations. The artefacts with LIA values are listed individually:

1) Near Eastern coins and objects: NEast

This includes the Byzantine objects (7 objects) and coins from the Asyut hoard that have Near East associations: Persian sigloi (Sardes) (3 coins), coins from Mallus or Caria (Anatolia) (5 coins) and Lycia (Anatolia) (2 coins).

2) Aegean and Cypriot coins: Aegean

Coins from the Asyut hoard: Athenian (14 coins), Orrescii (6 Coins), Corinth (9 coins), Lesbos (1 coin), Samos (5 coins), Thasos (4 coins), Acanthus (3 coins) and Salamis (Cyprus) (1 coin).

3) Aeginetan coins: Aeginetan

These 46 coins (38 with LIA) have been put in a separate group as they do not fall within one group based on LIA. Furthermore, with no silver sources of its own, Aegina is likely to have acquired silver from several sources (Gale et al., 1980).

4) Other coins:

Coins from Zankle (3 coins) and Messana (1 coin) (Sicily).

Table 1 shows the number of objects or coins which fall above and below the median of the iridium concentration for all the artefact data (44 ppb). The median was chosen as it better represents a skewed distribution (Fig. 1) than the mean. It can be seen that 135 out of 180 artefacts classified as Near Eastern lay above the median, i.e. 75% of all Near Eastern artefacts. The majority of the artefacts classified as Aegean, Aeginetan or Other, lay below the median. This is similarly reflected in the samples that have associated LIA data (Fig. 10) with 18 of the 102 plotted points (18%) having iridium values above 44 ppb Ir, in some cases over an order of magnitude higher. The majority (10 of the 18) of these elevated iridium levels are from the Near East group, 4 from the Aegean and 4 from the Aeginetan group. This suggests strongly that higher iridium levels are much more frequent in the silver-bearing ores of the Near East than those of the Aegean.

Fig. 10 also shows that several of these high iridium silver artefacts are coincident with ores that are about 65 million years old (as shown by the blue vertical dashed line), especially when it is considered that each point could have errors calculated in the Pb crustal age as high as ± 30 Ma due to 0.1% analytical errors propagated from LIA measurements; cf. Stos-Gale (2014). The elevated concentration of iridium in some samples is between 10 and 20 times the baseline level. Since such elevated levels of iridium in silver artefacts appear to be exceptional, it is possible that this is unique, with elevated levels of iridium coming from one single deposit (and possibly one mining area). It is proposed here that this mining area is in the Taurus mountain range. In other words, the 7 Byzantine objects, 2 Persian sigloi, 1 coin from Mallus or Caria, 1 Athenian coin, 2 coins from Corinth, 4 Aeginetan coins and 1 coin from Lesbos all derived from the same high-iridium, silver-bearing ore source. The Near Eastern artefacts and possibly the coin from Lesbos (which lies off the coast of Anatolia) fit well with such a scenario. Similarly, as mentioned earlier, Aegina has no silver deposits of its own and could therefore have acquired silver from a number of sources, including Anatolia. The two coins from Corinth and the coin from Athens are more problematic since both Corinth and Athens supposedly derived their silver from the galena ores of Laurion. However, these three coins have gold concentrations greater than 0.1 wt% (Corinthian 0.39 wt% and 0.26 wt%; Athenian 0.24 wt%), suggesting that they were not produced from a galena ore source, and possibly came from re-stamped coins of Near Eastern origin.

Fig. 11 shows traditional LIA ratio plots for ores in the Taurus mountains, Laurion ores, Athenian coins and silver objects with iridium values in excess of 44 ppb (Fig. 10). LIA values for some of the Sasanian objects have also been plotted, derived from the unpublished data of Meyers (Stos-Gale, 2001). These analyses were not plotted alongside their iridium values in Fig. 10 because different parts of the objects (made from different silver batches) were measured to determine compositions, while only one value was presented for the LIA. Nevertheless, from the 10 LIA values available for

the Sasanian objects described above, 7 are in excess of 44 ppb. The LIA values of these are also plotted in Fig. 11.

As expected, the Athenian coins are commensurate with the ores from Laurion. Silver with elevated levels of iridium have similar LIA ratios to ores from the Taurus mountain region, supporting that these objects originated from silver mined in this region.

Fig. 12 presents all data delineated into compositional groups based on gold (High: Au>0.1 wt%; Low: Au<0.1 wt%) and iridium (High: Ir > 44 ppb; Low: Ir < 44 ppb) levels. The HighAu-HighIr region contains Sasanian and Byzantine silver objects, including those classified as 'Sasanian Royal', as well as a number of coins of Near Eastern origin. This group has a wide range of crustal ages (about 150Ma), with no obvious central tendency. The one point identified as LowAu-HighIr is an individual coin that was analysed alongside the Asyut hoard but which has a different archaeological provenance (Wells hoard), and is potentially from a different mint (Figueira, 1998), which could suggest another ore source (Pb crustal age is 25Ma). The LowAu-LowIr group contains the Orrescii coins, the majority of the Athenian coins and a number of coins from Aegean and Aeginetan groups. Fig. 13 shows a histogram of the crustal ages for this LowAu-LowIr compositional group, highlighting that the majority are commensurate with the crustal ages associated with the ores of Laurion (Fig. 8). However, some of the coins in this group are aligned with a different population, with a higher crustal age (about 60Ma). This could suggest a low gold-low iridium ore source with relatively higher crustal ages than Laurion.

The HighAu-LowIr group contains Sasanian silver objects which were not classified as 'royal', and coins with gold concentrations higher than expectable from galena ore sources. It has a wide range of crustal ages (about 150Ma), without any obvious central tendency.

5. DISCUSSION

The scenario presented is that any ancient silver artefact with elevated levels of iridium, regardless of the chronology or find-site, will have silver that came from a single mining area - probably a mining area in the Taurus Mountains of southern Anatolia. The conservative lower limit of 44 ppb Ir is a reasonable indicator for silver from this source and the results of the meta-analysis indicate that most of the silver which ended up in Sasanian and Byzantine objects came from this high-iridium silver deposit. If the hypothesis is correct, the results also show that this deposit was being exploited at least 1000 years earlier to produce Near Eastern and Greek coins.

One issue with the Iridium-Pb crustal age plot (Fig. 10) is that not all of the silver laying above the iridium horizontal baseline fall on the vertical 65 million year line, as one might expect if all of the objects derive from the same silver source. Even considering that some of this data will have errors in the Pb crustal age, the very low crustal age of the Athenian-minted coin and the high crustal age of one of the Byzantine objects would seem difficult to reconcile with an origin in a single mining area. However, this and other issues mentioned above can be resolved by considering that, in those cases, exogenous lead from a different source was used as a collector to smelt the silver. This possibility is now addressed, while at the same time illustrating further the potential of the approach that considers compositional log-ratios alongside LIA data.

The large scatter in crustal ages observed in Fig. 9 is potentially due to variations in the ages within each silver-bearing ore body as well as between ore bodies (as seen, for example, in the variation in crustal ages of the Taurus mountain range - Fig. 7). However, another potential source of variability is related to the particular technological requirements associated to each ore mineralogy, and specifically the need (or not) to add exogenous lead as a silver collector. The Orrescii and Athenian

coins were probably derived from galena, which does not require lead to be added during the processing, as the silver is a trace element within the lead itself. In this case, the silver-bearing ore and the lead used to extract the silver will have the same crustal age, thereby resulting in a narrow range of crustal ages for the ore source as deduced from the object. This can explain why the Athenian and Orrescii coins have a relatively narrow range of crustal ages. A similar argument can be applied to pure cerussite sources, because of the intrinsic lead. However, the ores of the Taurus mountains are complex and variable, with some of them being more lead-rich than others (Yener et al., 1991). If lead was sometimes added to smelt and/or refine Near Eastern silver in order to act as a silver collector, the silver-bearing ore could derive from one location while the lead (and therefore the signature from which the Pb crustal age is calculated) could derive from another. In this scenario, a wide range of crustal ages would be measured even though the silver (and hence the iridium and gold) comes from one geological deposit. For example, high-iridium silver ore smelted with lead from Taurus 2A would result in silver with a high crustal age, while high-iridium silver ore smelted with lead from Taurus 1B would have a crustal age commensurate with the Athenian coin. By the same rationale, silver-bearing ore which lays close or on the 65 million year line probably had sufficient intrinsic lead to extract the silver, or lead was added from a deposit that was approximately the same age as the silver-bearing ore.

The logical extension of this argument is that the practice of adding lead would not have to have been confined to the high-iridium silver deposits identified above, but is more likely to have been common practice for those mining and extracting silver from the complex ores of Anatolia (from 475BCE, and probably much earlier). There is circumstantial evidence for this practice from the second millennium BC (Pernicka, 2014). Furthermore, evidence of the addition of lead to smelt silver-bearing ores has been found in Spain, where lead from Cartagena was added to silver-bearing ores from the Corta Lago mine of Rio Tinto by the Romans (Salkield, 1982). Slag from Phoenician levels at the same site suggests that exogenous lead was added even when the ores were sufficiently lead-rich to collect silver (Anguilano et al., 2009 ; Murillo-Barroso et al., 2016). This practice could explain why the Aeginetan coins have such a wide range of crustal ages: some silver came to Aegina from Laurion where it was stamped into Aeginetan coins (these coins have Pb Crustal ages in line with the silver from Laurion, <0.1 wt% Au as expected from galena, and lay on a line on the log-ratio plot which reflects the compositional variability of this mining area), while other silver came from various mines around Anatolia (including the deposit with high iridium levels) where the practice of adding lead to extract silver resulted in a range of crustal ages depending on the lead ore source exploited. This would present an almost intractable problem for lead isotope analyses, as determining the ore source a priori from an object would not only require knowledge of all the silver-bearing ore sources and lead ore sources, but would result in a multitude of scenarios due to the permutations of how they were combined (the result of which is perhaps evident in the wide spread of crustal ages for the Asyut hoard and Byzantine objects discussed above). The gold and iridium log-ratios, however, help us triangulate this issue.

A further reason for the wide range of crustal ages is the thorny issue of mixed silver. In this scenario, however, the linearity of the log-ratio plot would be altered as well as potentially exhibiting a wide range of crustal ages. The linearity of the Sasanian and Byzantine data suggests that the silver for these objects was not mixed. Similarly, the Orrescii coins and other coins in the LowAu-LowIr group appear to exhibit linear relationships, which suggests that the majority are from unmixed sources (in this case, also supported by the narrow range of crustal ages). Turning to the HighAu-LowIr group (Fig. 12), this group comprises coin data and Sasanian/Byzantine objects, both from non-galena sources; the Sasanian/Byzantine objects tend to lay on a line (Fig. 3) while the coin

data cover a broader range of log-ratio values. Fig. 14a shows the iridium concentration for this group vs. Pb crustal age for the data with LIA values (comprising coins from the Asyut hoard).

It is apparent that for the majority of data in this group, the iridium concentration is relatively invariant with crustal age. This suggests that the silver is not mixed and that the wide range of crustal ages is a consequence of the exploitation of many ore sources, the addition of lead from different locations to extract silver from these sources, or more likely, a combination of both. However, a convincing linear interaction is present in the upper part of the plot, which indicates that for these coins two sources with different crustal ages and iridium levels were mixed together. These data values are presented alongside their gold concentrations (Fig. 14b). Assuming the extreme points are the end members of a mixing line suggests that some of the coins which lay in the HighAu-LowIr group are a mixture of two types of silver: one with about 35 ppb Ir, 0.2 wt% Au and a crustal age of 12Ma and another with about 10 ppb Ir, 0.4 wt% Au and a crustal age of 144 Ma.

Evidence of mixing can also be observed in the HighAu-HighIr group. Although this group is made up of Sasanian and Byzantine objects and Near Eastern coins which predominantly lay on a relatively linear line on the log-ratio plot (Fig. 12), there are several coins in this group which deviate from this 'line'. Furthermore, a relatively linear interaction can be observed in Fig. 10, which is shown alongside the gold concentration in Fig. 14c. Again, mixing of two types of silver is suggested: one with about 35 ppb Ir, 0.35 wt% Au and a crustal age of 8Ma and another with about 365 ppb Ir, 0.8 wt% Au and a crustal age of 153 Ma.

The concordance of the iridium and gold values at low crustal ages for both the HighAu-HighIr and the HighAu-LowIr groups suggests strongly that one component of the silver mixture is the same for both groups (Fig. 14d), i.e. silver with about 35 ppb Ir, 0.2–0.35 wt% Au and a crustal age of between 8 and 12Ma. In the case of the HighAu-LowIr group, this silver was mixed subsequently with another silver which had a lower iridium concentration but a higher gold concentration. Conversely, for the HighAu-HighIr group, the silver was mixed with silver which had both higher iridium and gold concentrations. Considering that silver with the highest levels of iridium is likely to have come from one mining area with a crustal age of 65Ma (see Section 4 above), then the end member of the mixing line (with a crustal age of 153Ma) is likely to represent high-iridium silver (hence 65Ma) which was smelted using lead from a location with a high crustal age, i.e. exogenous lead dominates the LIA signatures from which the crustal age was calculated. Furthermore, it is also suggestive that the lead source used as a silver collector was common to both the HighAu-LowIr and HighAu-HighIr groups, as the end members have very similar crustal ages (144Ma and 153Ma, respectively). This could denote a lead mining area (perhaps Taurus 2A) where lead was extracted and used as a silver collector for the smelting of lead-poor silver-bearing ores.

6. CONCLUSIONS

One aim of the current work was to re-evaluate the legacy data available in the archaeological literature to determine whether iridium is an element that should be more often analysed for during archaeometallurgical investigations. The re-analysis indicates that the Ag-Au-Ir log-ratio sub-compositional plot based on the analysis of silver objects can help identify not only broad geological deposits but also mining areas within a deposit from which ancient silver was extracted. Combining this sub-compositional plot with LIA data through the Pb crustal age, delimits interpretations of the data in some circumstances. In situations where no exogenous lead has been added to act as a silver collector at a particular source, the crustal ages for artefacts will tend to fall within a narrow range, and the subcompositional data will lay on discrete lines (or clusters) on the log-ratio subcomposition plot. This provides a strong signature that may allow the location of the relevant silver ore to be

determined. Ore analyses are the focus of future work to ground-truth the utility of such signatures. When lead is added, the range of crustal ages can be high and it becomes much more difficult to delimit the ore source based on LIA, but the Ag-Au-Ir ratios can still be useful to demarcate groups that may correspond to silver sources. In any case, the combined approach piloted here, incorporating both chemical and isotopic data, helps identify with higher confidence cases where lead was added as a collector and/or silver was mixed (e.g. through recycling). This provides useful indicators for economic and technological behaviours of great archaeological significance, which have generally been assumed rather than proved. For the dataset investigated here, the practice of adding lead appears to have been a Near Eastern practice from at least as early as 475BCE and mixing silver was common in the Aegean during the same period.

An unexpected outcome of reanalysing the legacy data was that high levels of iridium appear to be confined to Near Eastern artefacts and coincident with ores aged about 65 million years. It is proposed that some of the silver-bearing ores mined in the Taurus mountain range had high levels of iridium, and this high-iridium signature can be traced in ancient silver objects.

ACKNOWLEDGMENTS

The authors would like to thank the LAHP/AHRC for funding the work of Jonathan Wood. The authors would also like to thank Francis Albarède for useful comments, Zofia Stos-Gale for providing some unpublished LIA data for Sasanian objects, as well as the editor and anonymous reviewers for constructive remarks.

References

- Aitchison, J., 1986. *The Statistical Analysis of Compositional Data*. Chapman and Hall, London.
- Aitchison, J., 2005. *A Concise Guide to Compositional Data Analysis*. 2nd Compositional Data Analysis Workshop. CoDaWork'05. Universitat de Girona, Girona.
http://ima.udg.edu/Activitats/CoDaWork05/A_concise_guide_to_compositional_data_analysis.pdf.
- Alard, O., Griffin, W.L., Lorand, J.P., Jackson, S.E., O'Reilly, S.Y., 2000. Non-chondritic distribution of the highly siderophile elements in mantle sulphides. *Nature* 407, 891-894.
- Albarède, F., Juteau, M., 1984. Unscrambling the lead model ages. *Geochim. Cosmochim. Acta* 48, 207-212.
- Albarède, F., Desaulty, A.-M., Blichert-Toft, J., 2012. A geological perspective on the use of Pb isotopes in archaeometry. *Archaeometry* 54, 853-867.
- Anguilano, L., Rehren, Th., Mueller, W., Rothenberg, B., 2009. Roman jarosite exploitation at Rio Tinto (Spain). In: *Archaeometallurgy in Europe 2007: Selected Papers from the 2nd International Conference, Aquileia, Italy, 17-21, June 2007*. Associazione Italiana di Metallurgia, Milan, pp. 21-29.
- Ayhan, A., 1984. Genetic comparison of lead-zinc deposits of Central Taurus. In: *Geology of the Taurus Belt, Proceedings 26-29, September 1983*. M.T.A., Ankara, pp. 335-342.
- Chalkias, S., Vavelidis, M., Schmitt-Strecker, S., Begemann, F., 1988. Geologische Interpretation der Bleisotopen verhältnisse von Erzen der Insel Thasos, der Ägäis und Nordgriechenlands. In: Wagner, G., Weisgerber, G. (Eds.), *Antike Edel- und Buntmetallgewinnung auf Thasos*, Deutsches Bergbau Museum, Bochum, pp. 59-74.

- Charles, J.A., 1985. Determinative mineralogy and the origins of metallurgy. In: Craddock, P.T., Hughes, M.J. (Eds.), *Furnaces and Smelting Technology in Antiquity*. British Museum Occasional Paper, vol. 48, pp. 21-28.
- Chayes, F., 1949. On correlation in petrography. *J. Geol.* 57, 239-254.
- Craddock, P.T., 1985. Three thousand years of copper alloys: from the Bronze Age to the industrial revolution. In: England, P.A., van Zelst, L. (Eds.), *Application of Science in Examination of Works of Art*, Boston: Museum of Fine Arts, pp. 59-67.
- Daryaee, T., 2009. *Sasanian Persia: the Rise and Fall of an Empire*, I. B. Tauris.
- Desaulty, A.-M., Telouk, P., Albalat, E., Albarede, F., 2011. Isotopic Ag-Cu-Pb record of silver circulation through 16th-18th century Spain. *PNAS* 108, 9002-9007.
- Figueira, T., 1998. *The Power of Money: Coinage and Politics in the Athenian Empire*. University of Pennsylvania Press.
- Freedman, D., Diaconis, P., 1981. On the histogram as a density estimator: L2 theory. *Z. Wahrscheinlichkeitstheorie Verw. Geb.* 57, 453-476.
- Gale, N.H., Gentner, W., Wagner, G.A., 1980. Mineralogical and geographical silver sources of archaic Greek coinage. In: Metcalf, D.M., Oddy, W.A. (Eds.), *Metallurgy in Numismatics I*, the Royal Numismatics Society, pp. 3-49.
- Gitler, H., Ponting, M., Tal, O., 2009. Athenian tetradrachms from tel Mikhal (Israel): a metallurgical perspective. *Am. J. Numismatics* 21, 29-49.
- Harper, P.O., Meyers, P., 1981. *Silver Vessels of the Sasanian Period*, Vol. 1. Princeton University Press. Royal Imagery, the Metropolitan Museum of Art.
- Hirao, Y., Enomoto, J., Tachikawa, H., 1995. Lead isotope ratios of copper, zinc and lead minerals in Turkey in relation to the provenance study of artifacts. In: Mikasa, H.I.H., Prince, T. (Eds.), *Essays on Ancient Anatolia and its Surrounding Civilizations*. Harrassowitz Verlag, Wiesbaden, pp. 89-114.
- Jessop-Price, M., 1980. The uses of metal analysis in the study of archaic Greek coinage: some comments. In: Metcalf, D.M., Oddy, W.A. (Eds.), *Metallurgy in Numismatics I*, The Royal Numismatic Society, pp. 50-54.
- L'Heritier, M., Baron, S., Cassayre, L., Tereygeol, F., 2015. Bismuth behaviour during ancient processes of silver-lead production. *J. Archaeol. Sci.* 57, 56-68.
- McKerrel, H., Stevenson, R.B.K., 1972. Some analyses of Anglo-saxon and associated oriental silver coinage. In: Hall, E.T., Metcalf, D.M. (Eds.), *Methods of Chemical and Metallurgical Investigation of Ancient Coinage* Hall, Royal. Numismatics Society, pp. 195-210.
- Meyers, P., 1992. Elemental compositions of the Sion treasure and other Byzantine silver objects. In: Boyd, S.A., Mango, M.M. (Eds.), *Ecclesiastical Silver Plate in Sixth Century Byzantium*, Dumbarton Oaks Research Library and Collection, Washington DC, pp. 169-190.
- Meyers, P., 2003. Production, distribution, and control of silver: information provided by elemental composition of ancient silver objects. In: *Patterns and Process: a Festschrift in Honor of Dr. Edward V. Sayre*, pp. 271-288.

- Meyers, P., van Zelst, L., Sayre, E.V., 1975. Major and trace elements in Sasanian silver, in: archaeological chemistry, *Advances in chemistry series*. Am. Chem. Soc. 138, 22-23.
- Moorey, P.R.S., 1985. *Materials and Manufacture in Ancient Mesopotamia: the Evidence of Archaeology and Art, Metals and Metalwork, Glazed Materials and Glass*, p. 237. Oxford: B.A.R. International Series.
- Muhly, J.D., 1973. Copper and Tin the Distribution of Mineral Resources and the Nature of the Metal Trade in the Bronze Age, *Transactions of the Connecticut Academy of Arts*, vol. 43. Hamden. Connecticut: Archon Books.
- Muhly, J.D., 1976. Supplement to Copper and Tin, *Transactions of the Connecticut Academy of Arts*, vol. 46. Hamden, Connecticut: Archon Books.
- Murillo-Barroso, M., Montero-Ruiz, I., Rafel, N., Hunt-Ortiz, M.A., Armada, X.-L., 2016. The macro-regional scale of silver production in Iberia during the First Millennium BCE in the context of Mediterranean contacts. *Oxf. J. Archaeol.* 35, 75-100.
- Nazafati, N., Pernicka, E., 2012. Early silver production in Iran. *Iran. Archaeol.* 3, 38-45.
- Oates, D., Oates, J., 1959. Ain Sinu: a Roman frontier post in northern Iraq. *Br. Inst. Study Iraq* 21, 207-242.
- Ogden, J.M., 1977. Platinum group metal inclusions in ancient gold artifacts. *J. Hist. Metallurgy Soc.* 11, 53-72.
- Pernicka, E., 1981. *Archaometallurgische Untersuchungen zur antiken Silbergewinnung in Laurion*. *Erzmetall* 36, 592-597.
- Pernicka, E., 2014. Provenance determination in archaeological metal objects. In: Roberts, B.W., Thornton, C.P. (Eds.), *Archaeometry in Global Perspective: Methods and Synthesis*. Springer.
- Pernicka, E., Bachmann, H.G., 1983. *Archaometallurgische Untersuchungen zur antiken Silbergewinnung in Laurion: III. Das Verhalten einiger Spurenelemente beim Abtreiben des Bleis*. *Erzmetall* 36, 592-597.
- Pernicka, E., Rehren, Th., Schmitt-Strecker, S., 1998. Late Uruk silver production by cupellation at Habuba Kabira, Syria. In: Rehren, Th., Hauptmann, A., Muhly, J.D. (Eds.), *Metallurgica Antiqua, Der Anschnitt, Beiheft 8*, Bochum, pp. 123-134.
- Pollard, A.M., Bray, P., 2015. Chemical and isotopic studies of ancient metals. In: Roberts, B.W., Thornton, C.P. (Eds.), *Archaeometry in Global Perspective: Methods and Synthesis*. Springer.
- Randle, K., Wellum, R., Whitley, J.E., 1973. Radiochemical determination of trace noble metals in silver artefacts. *J. Radioanalytical Chem.* 16, 205-214.
- Salkield, L.U., 1982. The roman and pre-roman slags at Rio Tinto Spain. In: Wertime, T.A., Wertime, S.F. (Eds.), *Early Pyrotechnology: the Evolution of the First Fire-using Industries*. Smithsonian Institution Press, Washington D.C., pp. 137-147
- Sayre, E.V., Yener, K.A., Joel, E.C., Barnes, I.L., 1992. Statistical evaluation of the presently accumulated lead isotope data from Anatolia and surrounding regions. *Archaeometry* 34, 73-105.
- Scott, D., 1990. A technical and analytical study of two silver plates in the collection of the J. Paul Getty museum. *J. Paul Getty Mus. J.* 18, 33-52.

Stacy, J.S., Kramers, J.D., 1975. Approximation of terrestrial lead isotope evolution by a two-stage model. *Earth Planet Sci. Lett.* 26, 207-221.

Stos-Gale, Z.A., 2001. The impact of the natural sciences on studies of hacksilber and early silver coinage. In: Balmuth, M.S. (Ed.), *Hacksilber to Coinage: New Insights into the Monetary History of the Near East and Greece*. The American Numismatic Society, New York, pp. 53-76.

Stos-Gale, Z.A., 2014. Silver vessels in the Mycenaean shaft graves and their origin in the context of the metal supply in the Bronze age Aegean. In: Meller, H.H., Risch, R., Pernicka, E. (Eds.), *Metals of power - Early gold and silver*, *Tagungen des Landesmuseums für Vorgeschichte Halle*, vol. 11, pp. 183-208, 1.

Stos-Gale, Z.A., Gale, N., 2009. Metal provenancing using isotopes and the Oxford archaeological lead isotope database (OXALID). *Archaeol. Anthropol. Sci.* 1, 195-213.

Stos-Gale, Z.A., Gale, N.H., Annetts, N., 1996. Lead Isotope Data from the Isotrace Laboratory, Oxford: Archaeometry data base 3, ores from the Aegean, part 1, *Archaeometry*, vol. 38, pp. 381-390.

Thomas, C.W., Aitchison, J., 2006. Log-ratios and geochemical discrimination of Scottish Dalradian limestones: a case study. In: Buccianti, A., Mateu-Figueras, G., Pawlowsky-Glahn, V. (Eds.), *Compositional Data Analysis in the Geosciences; from Theory to Practice*, Geological Society, vol. 264. Special Publications, London, pp. 25-41.

Tylecote, R.H., 1987. *The Early History of Metallurgy in Europe*. Longman, London.

van den Boogaart, K.G., 2013. Package 'compositions'.
<http://cran.rproject.org/web/packages/compositions/compositions.pdf>.

Wagner, G.A., Begemann, F., Eibner, C., Lutz, J., Ötzunal, Ö., Pernicka, E., Schmitt-Strecker, S., 1992. Archäometallurgische Untersuchungen an Rohstoffquellen des frühen Kupfers Ostanatoliens. *Jahrb. Des. Römisch-Germanischen Zentralmuseum Mainz* 36, 637-686 part 2.

Wertime, T.A., 1968. A metallurgical expedition through the Persian desert. *Science* 159, 927-935.

Wertime, T.A., 1973. The beginnings of metallurgy: a new look. *Science* 182, 875-887.

Yener, K.A., Özbal, H., 1986. The Bolkardag mining district survey of silver and lead metals in ancient Anatolia. In: Olin, J.S., Blackman, M.J. (Eds.), *Proceedings of the 24th International Archaeometry Symposium*. Washington DC. The Smithsonian Institution Press, pp. 309-320.

Yener, K.A., Özbal, H., 1987. Tin in the Turkish Taurus mountains: the Bolkardag mining district. *Antiquity* 61, 64-71.

Yener, K.A., Sayre, E.V., Joel, E.C., Özbal, H., Barnes, I.L., 1991. Stable lead isotope studies of central Taurus ore sources and related artifacts from Eastern Mediterranean chalcolithic and Bronze Age sites. *J. Archaeol. Sci.* 18, 541-577.

FIGURES

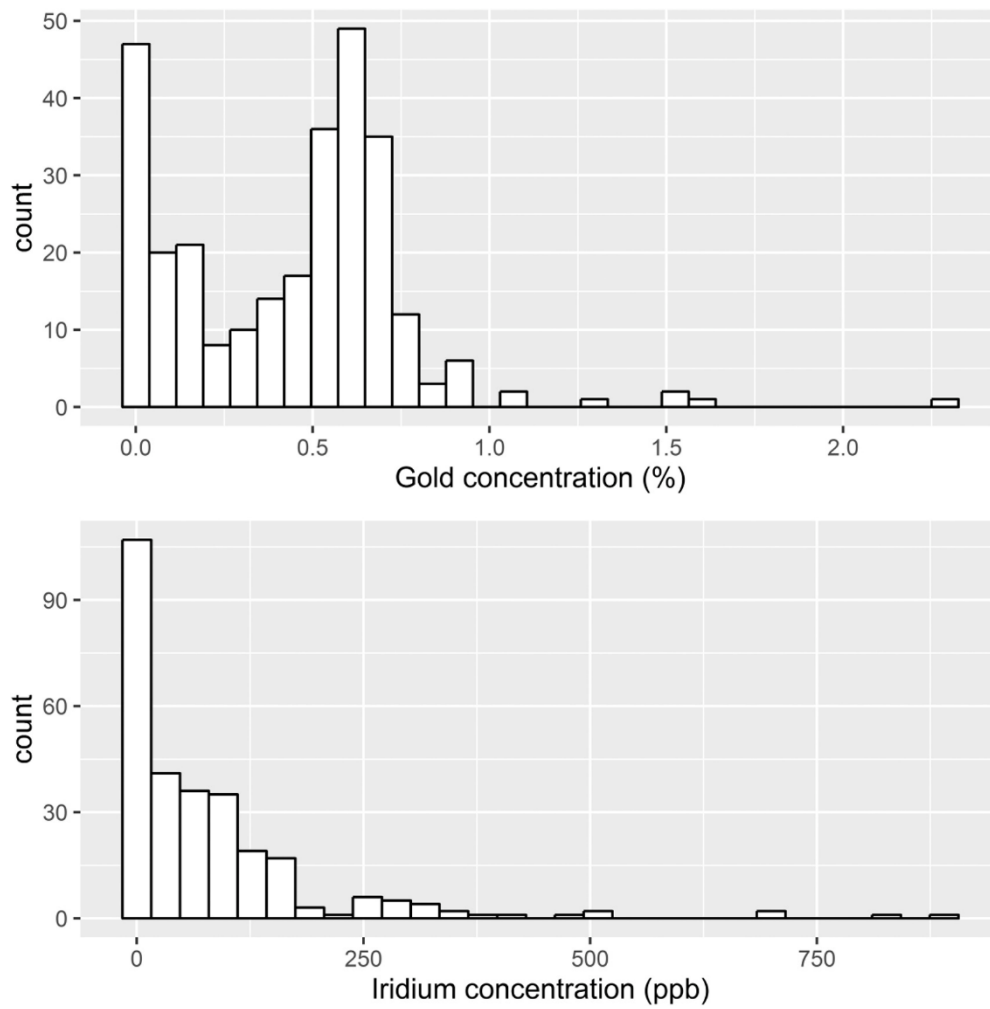


Figure 1. Frequency distribution histograms of the iridium (ppb) and gold (wt%) concentrations of the full dataset. The bin width was set using the Freedman-Diaconis rule (Freedman and Diaconis, 1981). Note that some objects were measured more than once because they had more than one part (e.g. foot, rim etc.). The histograms show that the gold concentration is bi-modal and that the iridium concentration has a skewed distribution with a median value of 44 ppb.

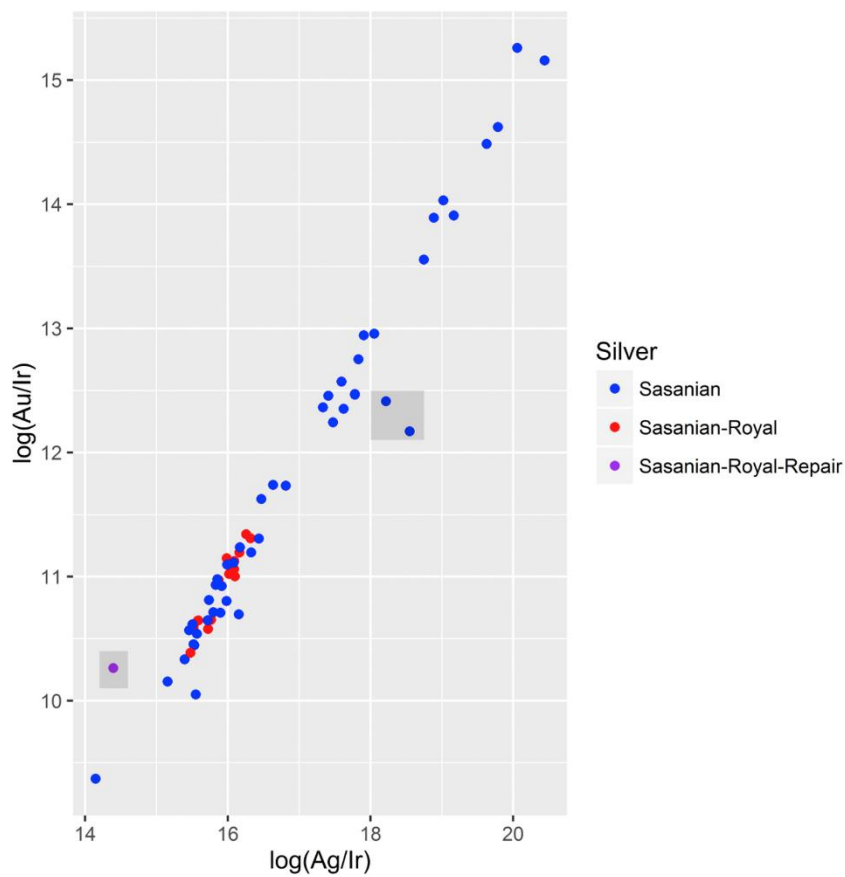
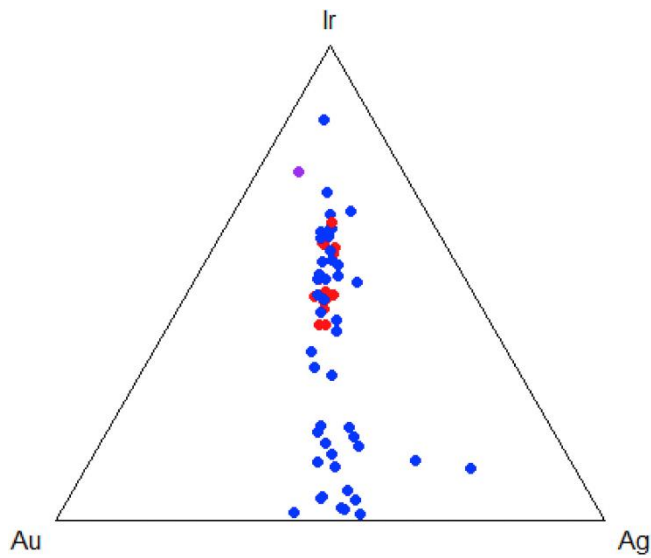


Figure 2. (a) Centred ternary for Sasanian silver data: Sasanian (●), Sasanian-Royal (●) and Sasanian-Royal-Repair (●). It is often typical to standardise the data in multivariate systems by scaling and centring the dataset in order to have a dimensionless, comparable variability. With transformed compositional data scaling is unnecessary as it already has a dimensionless scale (van den Boogaart, 2013). (b) Log-ratio plot for Sasanian silver data. Note that the clustering of the 'royal' silver suggests a mining area within the geological deposit while the repair and two points off-set from the relatively linear interaction suggest a different mining area and potentially a different ore type (highlighted). The overlap of some of the provincial objects with the royal objects could either suggest that these 'royal' mines were not restricted to the royal workshops or that these objects have been misidentified as provincial.

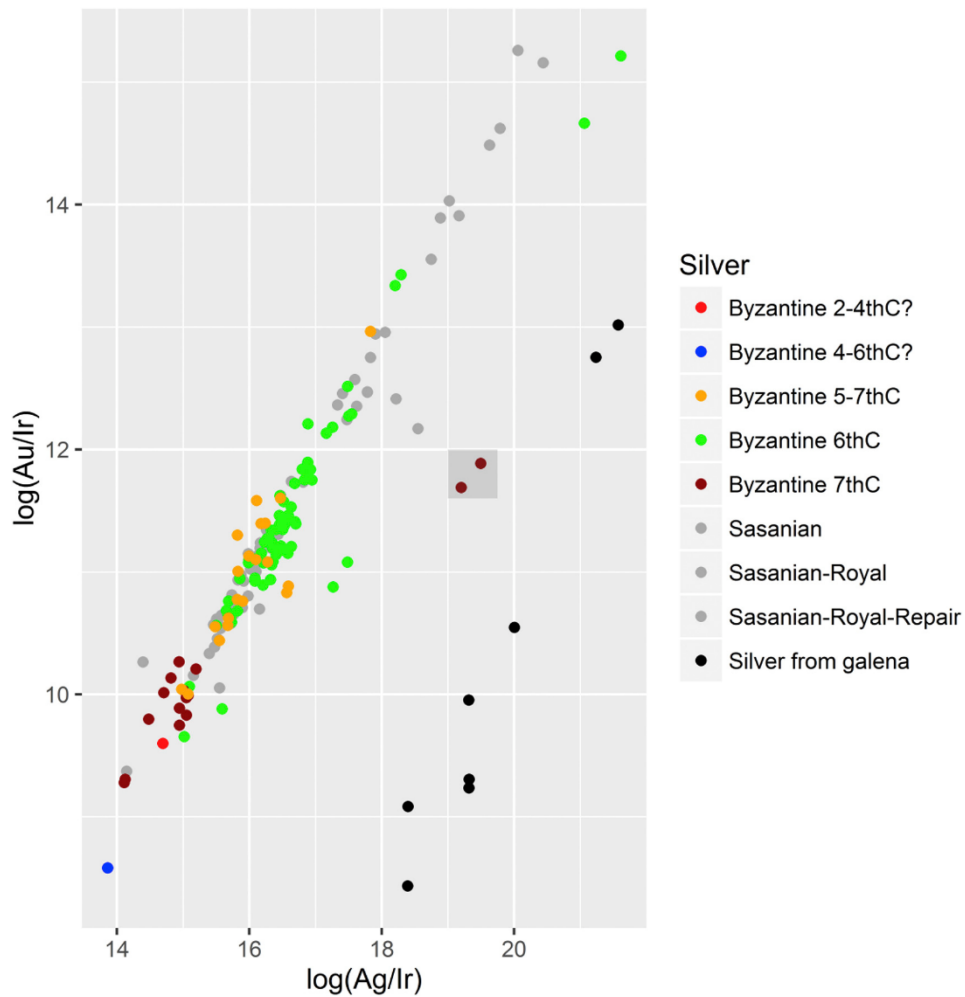


Figure 3. Log-ratio plot showing the sub-composition for Sasanian (in grey) and Byzantine silver objects as well as silver from two potential galena sources - 6 coins from Orrescii c. 5th C BC (Gale et al., 1980), and two early Islamic plates (Meyers, 2003). Note that these 'galena' points have a lower y-offset than the Sasanian/Byzantine data. The question marks for the Fisherman (2-4thC AD) and Philosopher's (4-6thC AD) plates highlight that these two objects were once suspected to be from the Renaissance period. The outlined grey box shows the 'Antioch Cross' which is clearly from a different geological deposit to the other objects in the Byzantine 7thC group.

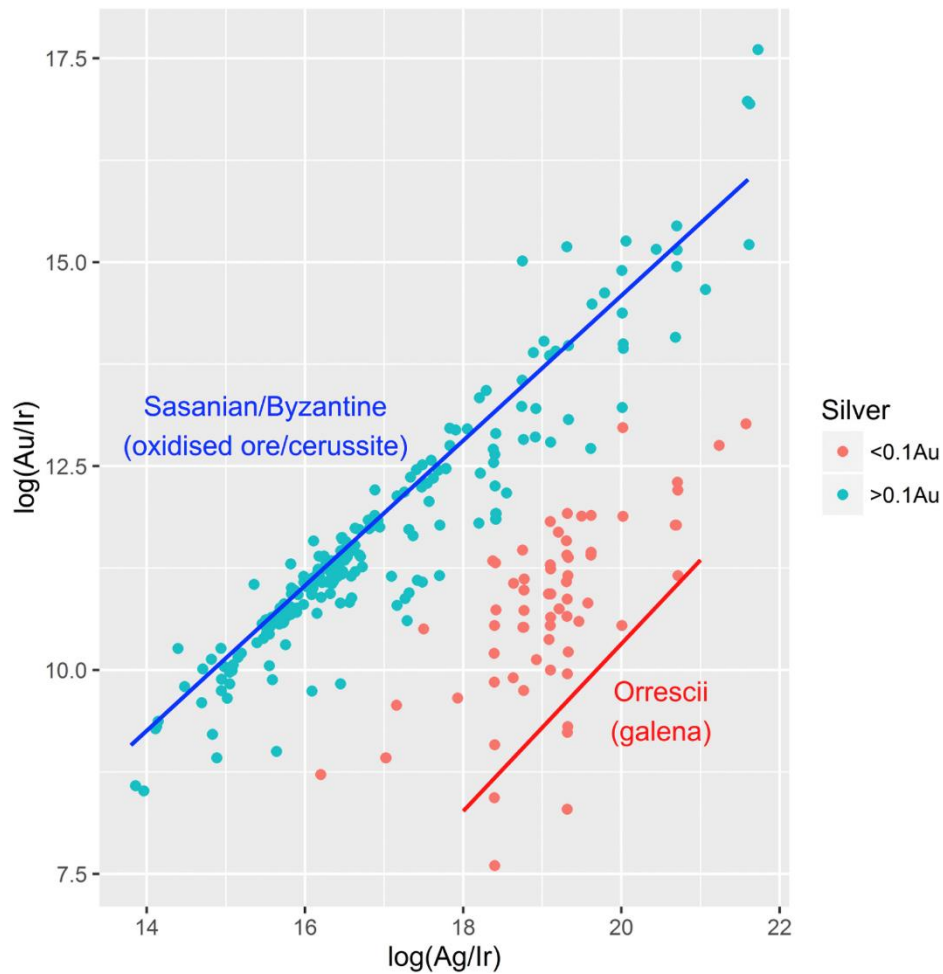


Figure 4. Log-ratio plot of the Ag-Au-Ir subcomposition showing all the Sasanian, Byzantine and Asyut data differentiated by gold concentration. The red line shows a fit just through the Orrescii data which are probably from a galena source. The blue line is a fit through both the Byzantine and Sasanian data shown in Fig. 3 which are probably from the complex oxidised silver-bearing ores of the Taurus mountains in southern Anatolia. The remainder of the points from the Asyut hoard have not been fitted as their ore source is less well identified. (For interpretation of the references to colour in this figure legend, the reader is referred to the web version of this article.)

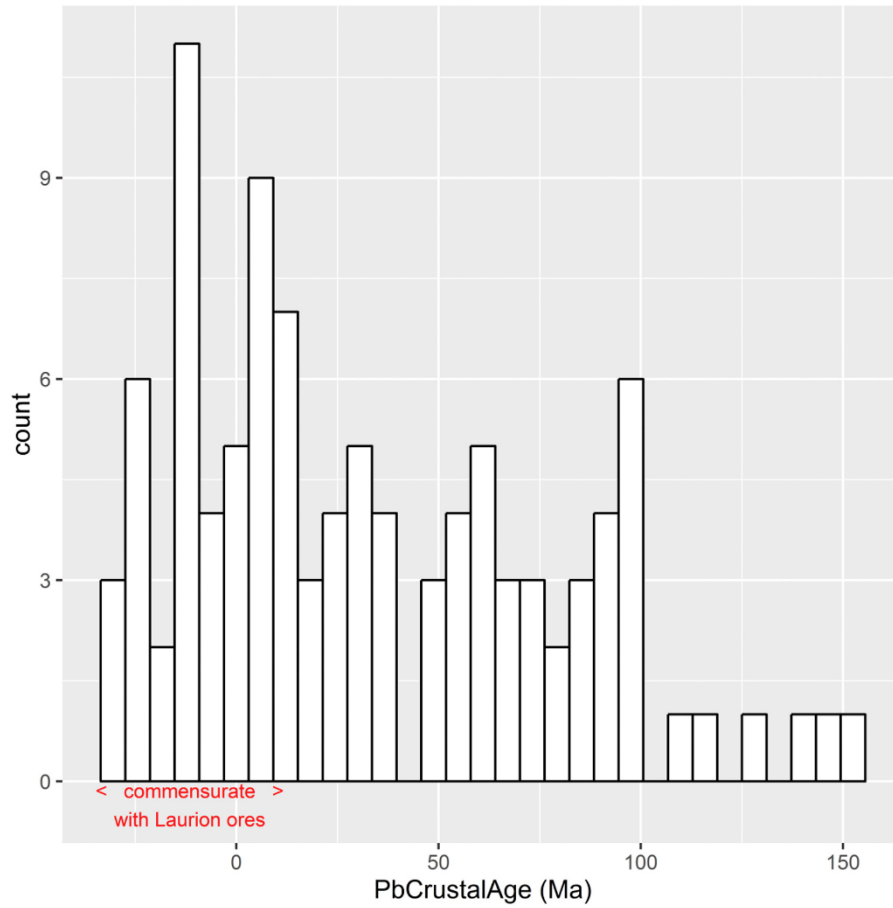


Figure 5. Frequency distribution histogram of the full dataset with LIA values. Pb crustal ages were calculated from the two-stage evolution model (Stacy and Kramers, 1975). The Freedman-Diaconis rule (Freedman and Diaconis, 1981) was used to set the bin width. Lower ages are commensurate with the ores from the Laurion mining area. Note the three higher frequency crustal ages of around 30, 60 and 95Ma.

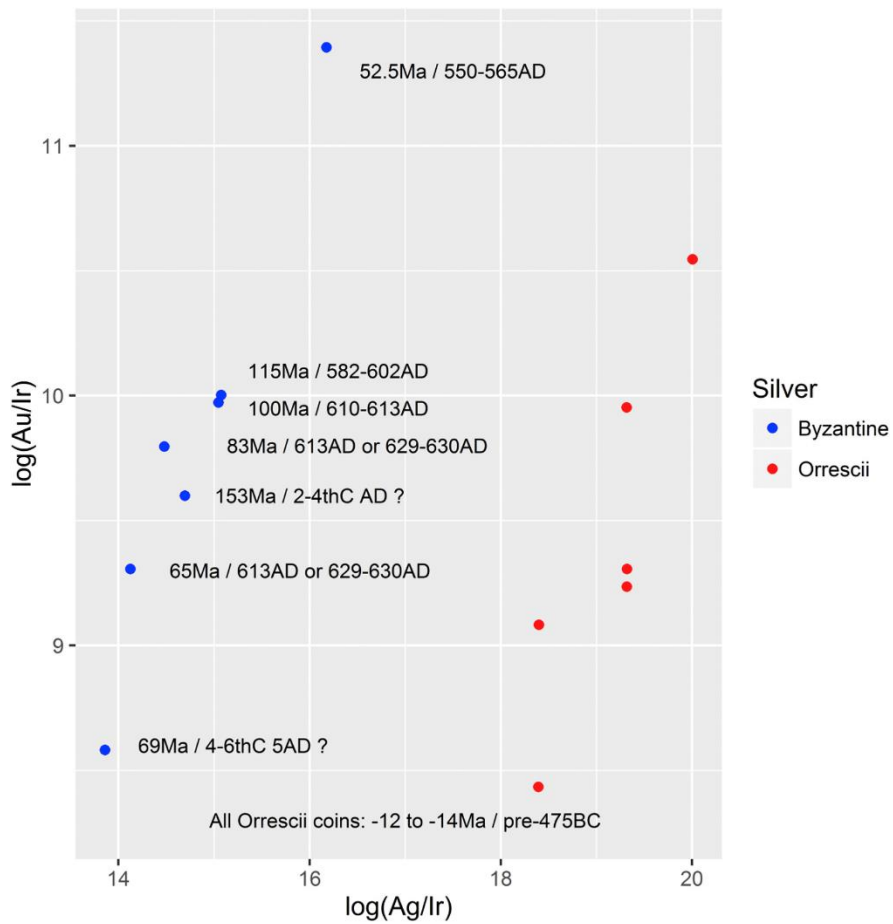


Figure 6. Log-ratio plot of the subcomposition showing the Byzantine and Orrescii data which have associated lead isotope values from which the Pb crustal age was calculated using the two-stage model (Desaulty et al., 2011). The Orrescii coins have a narrow range of crustal ages, while the Byzantine objects have a range of about 100 million years (Ma). The chronological ages of the silver objects/coins are also presented. The question marks for the Fisherman (2-4thC AD) and Philosopher's (4-6thC AD) plates highlight that these two objects were once suspected to be from the Renaissance period.

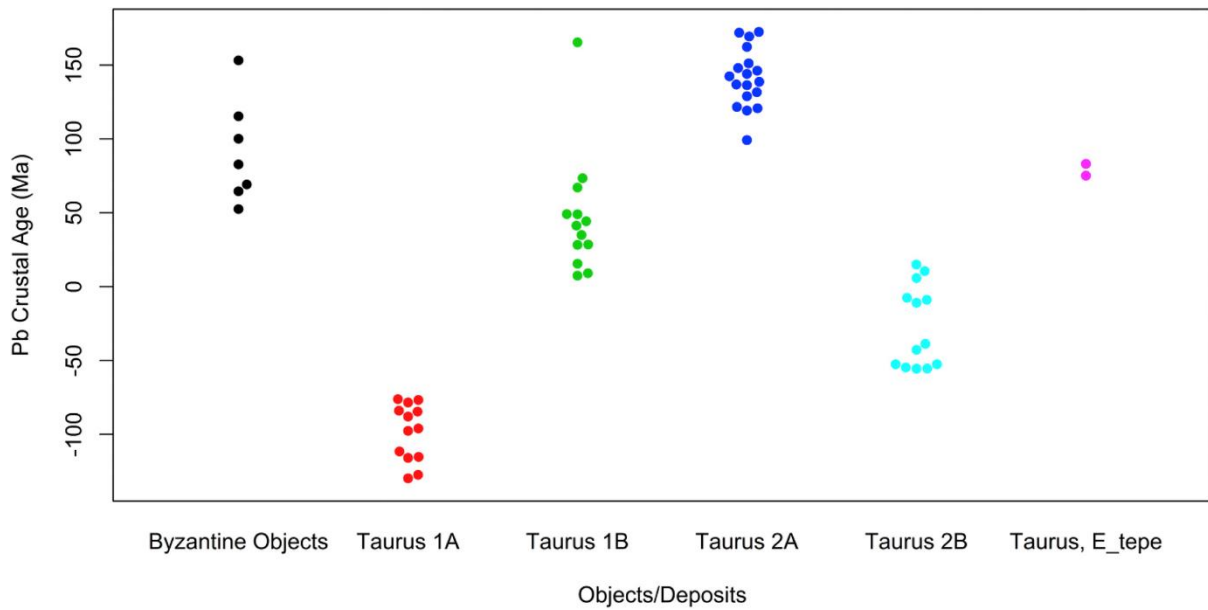


Figure 7. Beeswarm plot of Pb crustal age of ores from the Taurus mountains in southern Anatolia and Byzantine objects (LIA data from *Yener et al., 1991; Wagner et al., 1992; Hirao et al., 1995*).

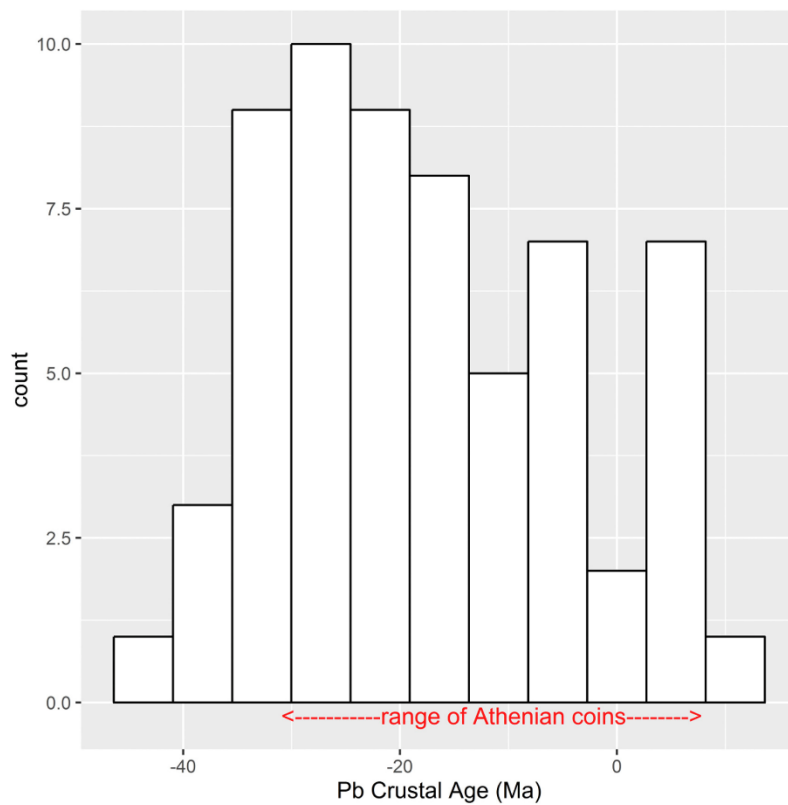


Figure 8. Frequency distribution histogram showing the range of Pb crustal age (Ma) calculated from lead isotope ratios from Laurion ores at 15 sites using a two-stage evolution model (*Stacy and Kramers, 1975*). LIA data from *Stos-Gale et al., 1996; Chalkias et al., 1988*. The Freedman-Diaconis rule (*Freedman and Diaconis, 1981*) was used to set the bin width. The crustal age of the ore deposit is commensurate with the Laurion cluster observed in *Fig. 8* from the Asyut coin data.

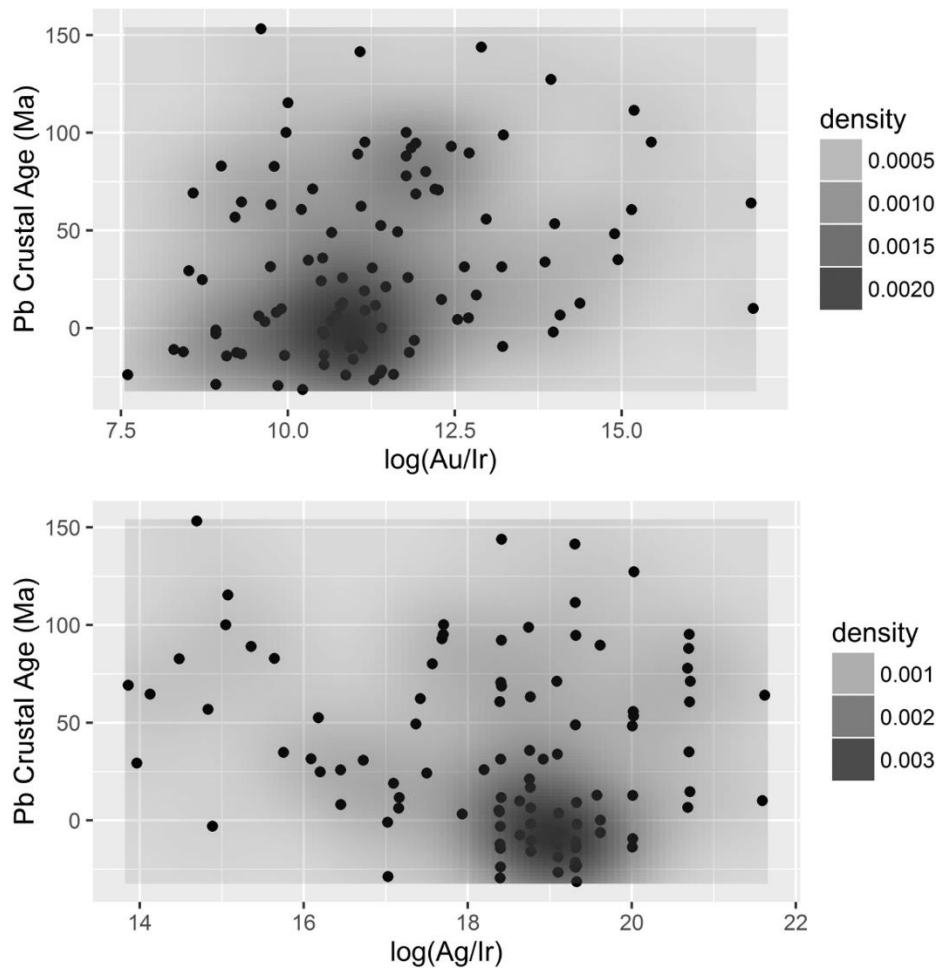


Figure 9. Kernel density plots for the Asyut coin data, where the shading corresponds to the smallest region which contains the respective probability. (top) Pb Crustal Age (Ma) vs Log (Au/Ir): Two regions of high density are visible. Note that the central value and spread of data in the lower region is similar to the range of crustal ages determined from coins from the Laurion mint and the range of Pb crustal ages from the Laurion ores. The higher region has a Pb Crustal Age commensurate with several ore bodies in the Aegean, and further afield. (bottom) Pb Crustal Age (Ma) vs Log (Ag/Ir) showing only high density in the lower region of the plot.

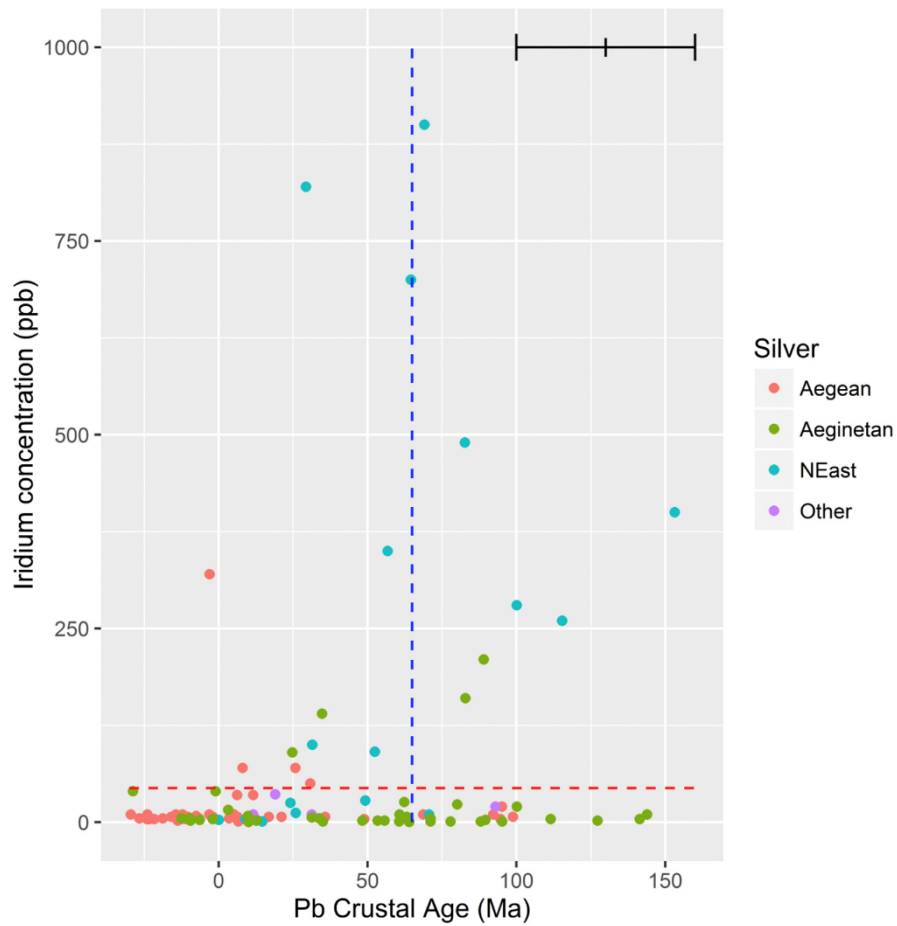


Figure 10. Iridium concentration (ppb) vs Pb crustal age (Ma) for all data with LIA values. The dataset is disaggregated into 4 groups based on geography (Table 1). The majority of samples which lay above the horizontal baseline (determined from the median of the whole dataset) are of Near Eastern origin. A number of samples cluster around 65 million years (vertical blue line). The error bar is $\pm 30\text{Ma}$, determined from the analytical error in the LIA measurements (Stos-Gale, 2014). Note the suggestion of linearity in the points increasing from lower to higher crustal ages (see Fig. 14). (For interpretation of the references to colour in this figure legend, the reader is referred to the web version of this article.)

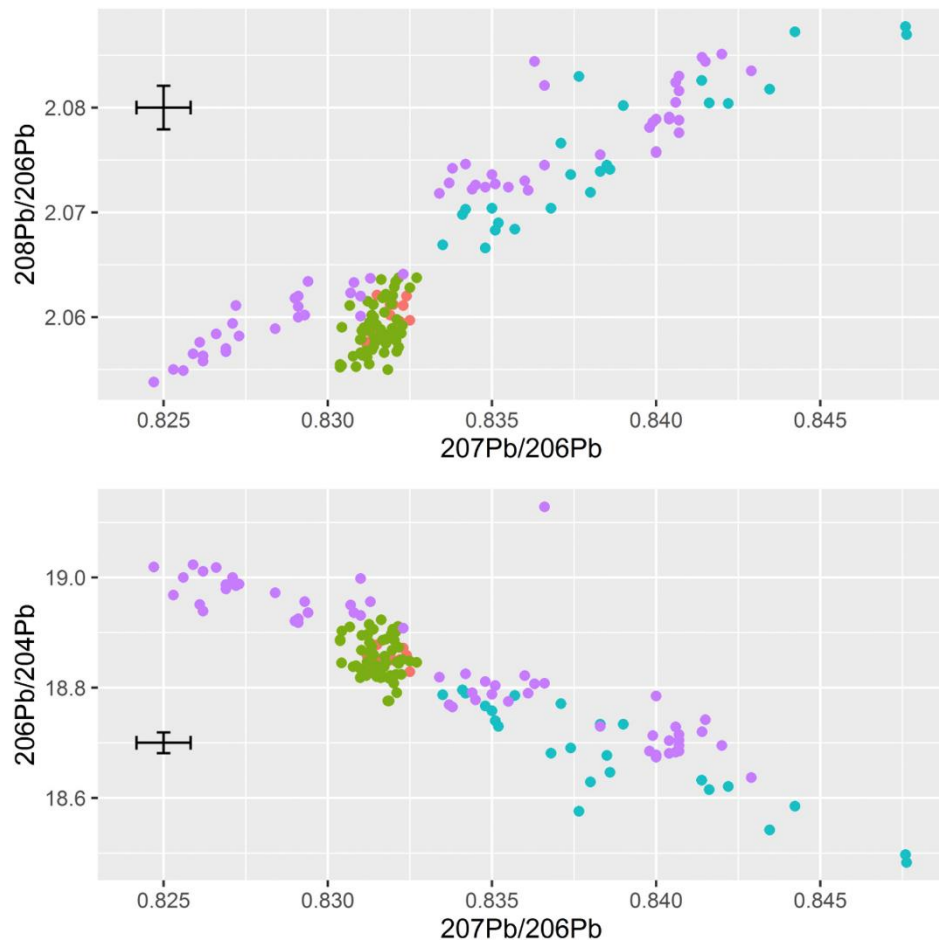


Figure 11. LIA ratio plots showing ores from Laurion (■) and the Taurus Mountains (■) alongside Athenian coins (●) and silver objects with iridium greater than 44 ppb (■). Error bars show the analytical errors ($\pm 0.1\%$).

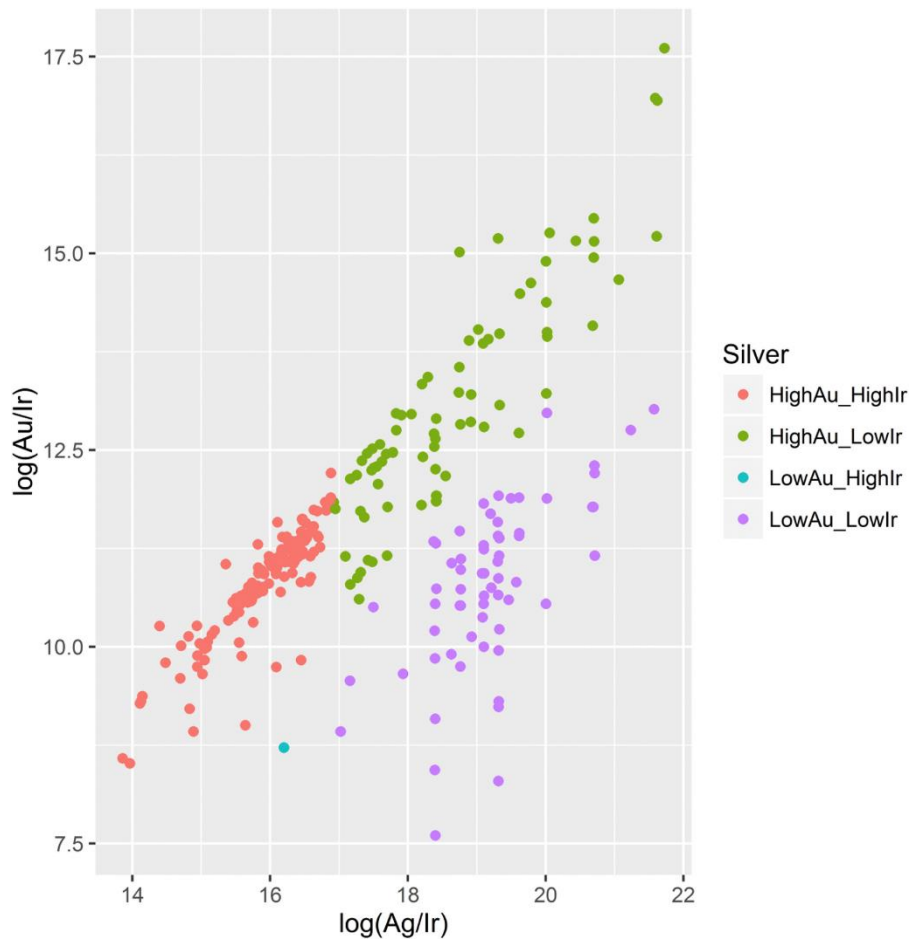


Figure 12. Log-ratio plot of all the data delineated by gold and iridium concentrations: High gold - $\text{Au} > 0.1 \text{ wt\%}$; Low gold - $\text{Au} < 0.1 \text{ wt\%}$; High Iridium - $\text{Ir} > 44 \text{ ppb}$; Low Iridium - $\text{Ir} < 44 \text{ ppb}$.

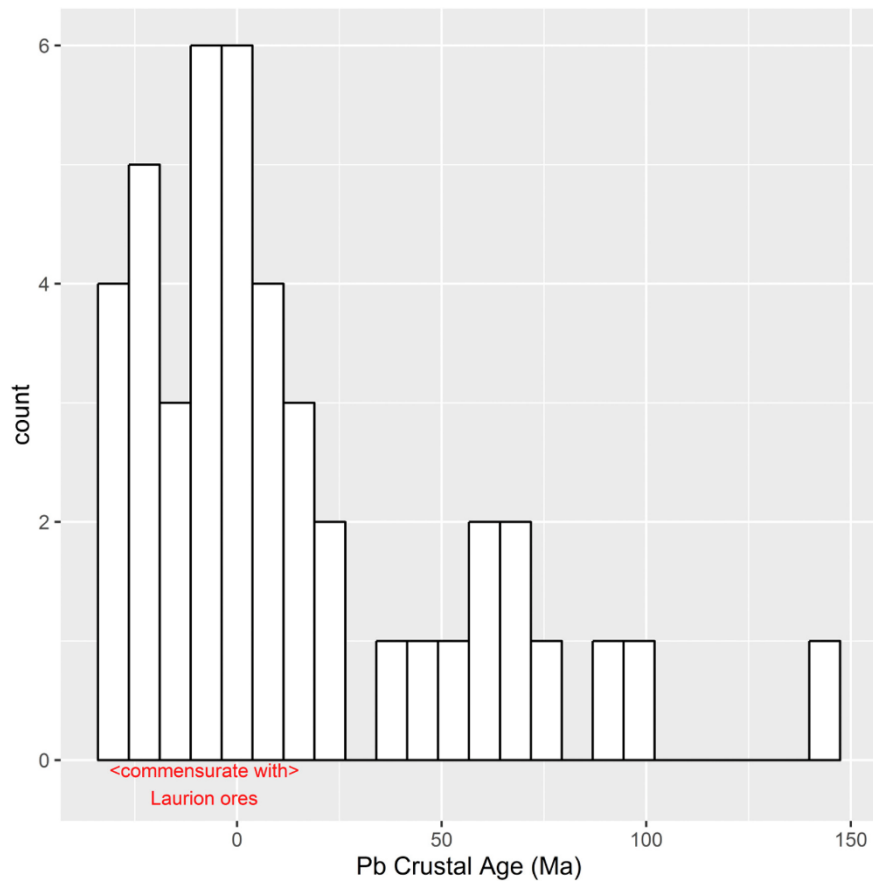


Figure 13. Frequency distribution histogram of Pb crustal ages (Ma) for LowAu-LowIr group. The Freedman-Diaconis rule (Freedman and Diaconis, 1981) was used to set the bin width. Lower crustal ages are commensurate with Laurion ores. A peak around 60Ma suggests that another silver source is present within this group.

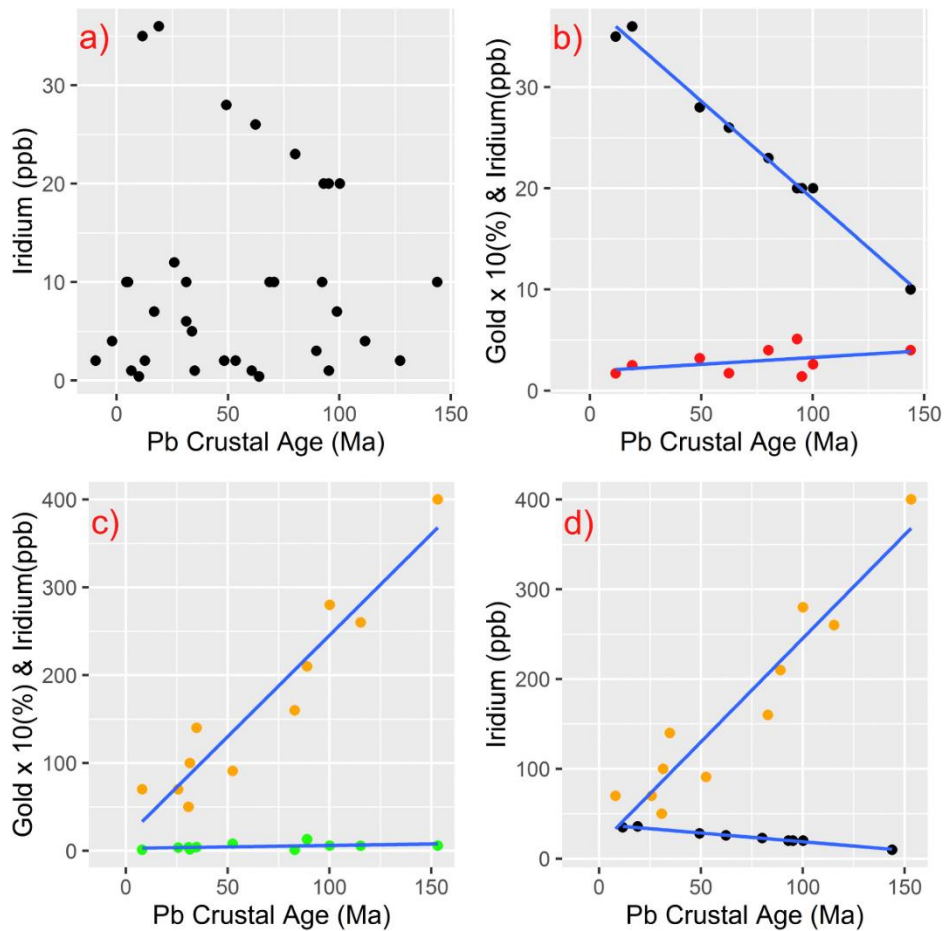


Figure 14. (a) Iridium concentration (ppb) vs Pb crustal age (Ma) for the HighAu-LowIr group with associated LIA values. Note that data in the upper part of the plot exhibit a potential linear relationship. (b) Iridium (ppb) (black) and gold (%x10) (red) concentrations vs Pb crustal age (Ma) for the data from the HighAu-LowIr group exhibiting linearity in Fig. 14a. (c) Iridium (ppb) (yellow) and gold (%x10) (green) concentrations vs Pb crustal age (Ma) for the data from the HighAu-HighIr group exhibiting linearity in Fig. 10. (d) Iridium (ppb) concentrations vs Pb crustal age (Ma) for the data from the HighAu-HighIr (yellow) and HighAu-LowIr (black) groups. Note the coincidence in the iridium values at low crustal ages suggesting that this end member of the mixing line was the same for silver from both groups. Note also that the crustal ages of the high end members of both groups are very similar. (For interpretation of the references to colour in this figure legend, the reader is referred to the web version of this article.)

TABLES

GROUP	Above median (>44 ppb Ir)		Below median (<44 ppb Ir)	
	With LIA	All	With LIA	All
Near East	10/17 (59%)	135/180 (75%)	7/17 (41%)	45/180 (25%)
Aegean	4/43 (9%)	4/50 (8%)	39/43 (91%)	46/50 (92%)
Aeginetan	4/38 (11%)	4/46 (9%)	34/38 (89%)	42/46 (91%)
Other	0/4 (0%)	0/7 (0%)	4/4 (100%)	7/7 (100%)

Table 1. Iridium levels, separated into geographical groups, of the number of samples out of the total number of samples ($n = 283$) and those with LIA values ($n = 102$), which lay above and below the median of the whole dataset ($Ir_{median} = 44$ ppb). The data with LIA values are plotted in [Fig. 12](#).